Physica E 45 (2012) 86–96

Contents lists available at SciVerse ScienceDirect

Physica E

journal homepage: www.elsevier.com/locate/physe

Transverse wave propagation in elastically confined single-walled carbon nanotubes subjected to longitudinal magnetic fields using nonlocal elasticity models

Keivan Kiani *

Department of Civil Engineering, Islamic Azad University, Chalous Branch, Chalous, P.O. Box 46615-397, Mazandaran, Iran

HIGHLIGHTS

- Transverse wave propagation in SWCNTs under axial magnetic field is examined.
- Nonlocal Rayleigh, Timoshenko, and higher-order beams are employed.
- The characteristic relations for the proposed models are derived.
- The explicit expressions of frequencies, phase, and group velocities are obtained.
- The role of crucial factors on the characteristics of propagated waves is explored.

GRAPHICAL ABSTRACT

The influence of longitudinal magnetic field on the characteristics of both flexural and shear waves in SWCNTs embedded in an elastic matrix is of concern. The problem is studied by using nonlocal Rayleigh, Timoshenko, and higher-order beam theories.

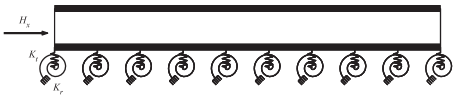

ARTICLE INFO

Article history:
Received 26 December 2011
Received in revised form
29 June 2012
Accepted 16 July 2012
Available online 24 July 2012

ABSTRACT

Lateral wave propagation in an elastically confined single-walled carbon nanotube (SWCNT) experiences a longitudinal magnetic field is examined using nonlocal Rayleigh, Timoshenko, and higher-order beam theories. The SWCNT is modeled via an equivalent continuum structure (ECS) and its interaction with the surrounding elastic medium is simulated via lateral and rotational continuous springs along its length. For the proposed models, the dimensionless governing equations describing transverse vibration of the SWCNT are constructed. Assuming harmonic solutions for the propagated sound waves, the dispersion equation associated with each model is obtained. Subsequently, the explicit expressions of the frequencies as well as the corresponding phase and group velocities, called characteristics of the waves, are derived for the proposed models. The influences of the slenderness ratio, the mean radius of the ECS, the small-scale parameter, the longitudinal magnetic field, the lateral and rotational stiffness of the surrounding matrix on the characteristics of flexural and shear waves are explored and discussed.

1. Introduction

From quantum physics point of view, the dynamical behavior of single-walled carbon nanotubes (SWCNTs) in magnetic fields has been of concern of scientific communities during the recent decade [1–5]. In the case of a magnetic field parallel to the nanostructure axis, it is predicted that the band of the nanostructure alters drastically due to the Aharonov–Bohm phase [6] generated around the circumference of the nanostructure [7]. The band-gap is expected to vibrate between zero and a predictable value [8]. Further, a transverse magnetic field leads to a distinctly different behavior: the zero-field band structure with one-dimensional van Hove singularities gradually changes into a Landau-level spectrum as the magnetic field increases [8]. The large diamagnetic susceptibility for transverse magnetic fields applied to graphene sheets would result in highly anisotropic

* Tel.: +98 191 2223796; fax: +98 191 2220536.
E-mail addresses: k_kiani@iauc.ac.ir, keivankiani@yahoo.com

1386-9477/$ - see front matter © 2012 Elsevier B.V. All rights reserved.
http://dx.doi.org/10.1016/j.physe.2012.07.015

magnetic susceptibilities of SWCNTs and originates magnetic alignment of them, which has been supported by experimentally observed data as well [9,10].

From applied mechanics point of view, when a SWCNT is deformed in a magnetic field, the Lorentz force is exerted on each considered element of its body. It implies that the vibration of the SWCNT would be surely influenced by the applied magnetic field. The directions of the applied forces on the deformed SWCNT are determined based on the Maxwell's equations as well as Lorentz's body forces formula. Therefore, altering vibrational characteristics of a SWCNT in a desired direction would be possible by applying appropriately directional magnetic fields. Recent experiments also show that SWCNTs could be aligned suitably under an electro-magnetic field [11–14]. Such evidences are proposing SWCNTs as suitable nanostructures for nano-electro-mechanical systems (NEMS), nanosensors, and nanodetectors in which the control of their frequencies is of great importance. As a result, development of appropriate models for predicting the vibration behaviors of SWCNTs under applied magnetic fields would be beneficial to the designers of the above-mentioned nanodevices.

To date, the theoretical aspects of free longitudinal and transverse vibrations of CNTs [15–22], sound wave propagation within CNTs [23–29], fluid flow-induced vibration in CNTs [30–37], and generated vibrations within CNTs due to a moving nanoparticle [38–42] have been fairly well studied using continuum models. However, there are a few works on the effect of longitudinal and lateral magnetic fields on the vibration characteristics of CNTs. Using a shell model in the framework of classical continuum mechanics, Wang et al. [43] studied the influence of axial magnetic field on wave propagation in MWCNTs embedded in an elastic medium. It was shown that for the so-called critical frequencies, the velocity of wave propagation jumps down considerably. Moreover, the velocity of wave propagation in CNTs increases with axial magnetic field in some frequency regions. Li et al. [44] investigated the effect of transverse magnetic field on vibration behavior of MWCNTs. Through consideration of van der Waals (vdW) interaction forces between each two layer and the applied Lorentz force on each layer, the coupled equations of motion of MWCNTs were obtained. The results showed that the lowest frequency of the MWCNTs decreases nonlinearly with applied transverse magnetic field while the highest frequency remains unchanged. For a transverse magnetic field larger than a certain value, the two walls of MWCNTs exhibit the radial and longitudinal vibration modes with a coaxial pattern. Wang et al. [45] proposed an analytical method to study the effect of vdW interaction forces on the dynamic characteristics of MWCNTs embedded in an elastic matrix under a lateral magnetic field. Each layer of the MWCNT is assumed to behave like an elastic shell which is interacted with its two adjacent layers through the vdW forces. It was reported that the existing vdW forces would result in a decrease of the lowest frequency and an increase of the highest frequency of the MWCNTs under a transverse magnetic field. It was also stated that the effect of rigorous vdW on magneto-elastic vibrations of MWCNTs relies on the level of the transverse magnetic field as well as the stiffness of the surrounding matrix.

All the above-mentioned works were dealing on the effects of magnetic fields on vibration characteristics of CNTs in the context of classical continuum theory. In study vibration characteristics of nanostructures, the interatomic bond plays a vital role and such an effect should be appropriately incorporated into the constitutive equations. The traditional (or classical) continuum mechanics does not consider the inter-atomic bond lengths in the constructed governing equations. One way to overcome such a deficiency of the classical continuum theory is to employ an atomistic-based approach for analyzing of the problem. The major advantageous of such a model is that the effects of all inter-atomic bonds could be taken into account through appropriate potential functions; however, the user of such a model should pay the expenditures of the huge amount of computational efforts and the human resources as well. Therefore, some sophisticated continuum theories have been developed during the last century to take into account the effect of small-scale parameter. Among all developed continuum models, a fairly simple form of the nonlocal continuum mechanics of Eringen [46–48] has been gained much popularity in the scientific communities. Maybe the main reason of this fact is that such a model could incorporate the inter-atomic bond in its formulations via a so-called factor, small-scale parameter. Due to such a simplification, some researchers have shown that such a considered small-scale parameter by this model is geometry dependent [49]. In this work, the sensitivity of the characteristics of the propagated transverse waves in SWCNTs to the small-scale parameter under different levels of axially applied magnetic field is also of concern.

As it is seen in the literature, the effect of longitudinal magnetic field on the characteristics of the laterally propagated waves in elastically confined SWCNTs to date has not been made known methodically. Herein, since only lateral vibration of SWCNTs is of particular concern, among various types of structural models, beams are employed in the context of nonlocal continuum theory of Eringen. Some characteristics of the propagated waves within a SWCNT including shear and flexural frequencies as well as the corresponding phase and group velocities are derived when the SWCNT is surrounded by an elastic matrix and experiences an axial magnetic field as well. The outline of this paper is as follows. The description of the problem and the made assumptions are given in Section 2. Evaluation of the induced forces within the SWCNT due to a longitudinal magnetic field is presented in Section 3. In Sections 4–6, the equations of motion describing transverse vibration of SWCNTs under an axial magnetic field based on the nonlocal Rayleigh beam theory (NRBT), nonlocal Timoshenko beam theory (NTBT), and nonlocal higher-order beam theory (NHOBT) are obtained, respectively. Further, the analytical expressions of frequencies, phase velocities, and group velocities of the shear and flexural waves are presented for the proposed models. Section 8 gives a fairly comprehensive parametric study to assess the influence of the crucial parameters on the frequencies, phase velocities, and group velocities of both shear and flexural waves. In the conclusion, the major obtained results are provided.

2. Assumptions and definition of the problem

Consider an equivalent continuum structure (ECS) for the SWCNT as shown in Fig. 1. The ECS is a hollow circular cylindrical solid structure whose mean radius, r_m, and length, l_b, are similar

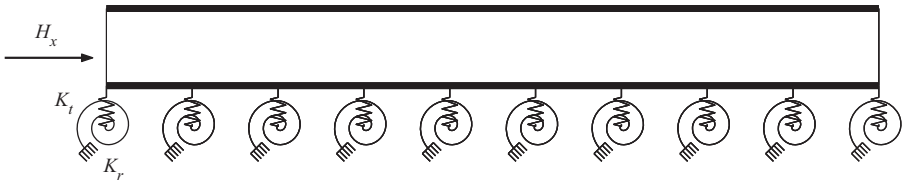

Fig. 1. An elastically confined SWCNT subjected to an axial steady magnetic field.

to those of the SWCNT and most of its frequencies are close to those of the SWCNT which are calculated via an appropriate atomistic-based approach. Therefore, it would be a suitable alternative for vibration analyses of SWCNTs since atomic techniques are commonly time-consuming and labor intensive. The interaction of the SWCNT with its surrounding elastic medium is modeled by laterally and rotationally continuous springs, which are attached to the ECS along its length (see Fig. 1). The constants of the transverse and rotational springs are denoted by K_t and K_r, respectively. The elastically confined SWCNT undergoes a longitudinal magnetic field, H_x.

This paper aids to investigate transverse wave propagation within the SWCNT under above-mentioned conditions. For this purpose, it is assumed that the SWCNT behaves like a perfectly conducting beam structure. In order to take into account the effect of the small-size of the SWCNT, the nonlocal continuum theory of Eringen [47,48] is employed. To explore the problem under study, the most famous beam models (e.g., Rayleigh, Timoshenko, and higher-order beam theories) are implemented. Using NRBT, NTBT, and NHOBT, the equations of motion describing the lateral vibration of SWCNTs should be constructed. To this end, the effect of the applied longitudinal magnetic field on the ECS should be appropriately modeled. In the next section, we proceed in determining the exerted body forces of the magnetic fields on the ECS modeled by various nonlocal beam theories.

3. Generated forces within the ECS due to a longitudinal magnetic field

Assume that the magnetic permeability of the ECS, ϱ, would be equal to the magnetic permeability of the surrounding medium. By neglecting displacement current density, the governing electrodynamic Maxwell's equations for a perfectly conducting ECS are stated as [50]

$$\begin{aligned}&\mathbf{J}=\nabla\times\mathbf{h},\\&\varrho\dot{\mathbf{h}}+\nabla\times\mathbf{e}=\mathbf{0},\\&\mathbf{e}=-\varrho\dot{\mathbf{u}}\times\mathbf{H},\\&\nabla\cdot\mathbf{h}=0,\end{aligned}\tag{1}$$

where $\mathbf{J}$ is the current density, $\mathbf{e}$ is the perturbation of electric field vector, $\mathbf{u}$ is the displacement field vector of the ECS, $\mathbf{H}$ is the magnetic field vector, ∇ is the Laplacian operator, and the over dot sign denotes the differentiation with respect to the time. The exerted body force vector on the ECS due to the applied magnetic field, $\mathbf{f}_b$, is evaluated from [50]:

$$\mathbf{f}_b=\varrho\mathbf{J}\times\mathbf{H},\tag{2}$$

where $\mathbf{f}_b$ is also called Lorentz's force vector. As it is seen in Eqs. (1) and (2), the interaction between the generated displacements within the ECS and the applied magnetic field would result in Lorentz body force vector. The longitudinal and transverse displacements within the ECS based on the Rayleigh, Timoshenko, and high-order beam theories are given by

$$\begin{aligned}&u_x^R(x,z,t)=u^R(x,t)-zw^R_{,x}(x,t);\quad u_z^R(x,z,t)=w^R(x,t),\\&u_x^T(x,z,t)=u^T(x,t)-z\theta^T(x,t);\quad u_z^T(x,z,t)=w^T(x,t),\\&u_x^H(x,z,t)=u^H(x,t)-z\psi^H(x,t);\quad u_z^H(x,z,t)=w^H(x,t),\end{aligned}\tag{3}$$

where u_x^R/u_z^R, u_x^T/u_z^T, and u_x^H/u_z^H denote the longitudinal/transverse displacement fields of the Rayleigh, the Timoshenko, and the higher-order beams, respectively. Furthermore, u^R, u^T, and u^H, in order are the longitudinal displacements of the neutral axis of the Rayleigh, Timoshenko, and higher-order beams. In the case of a longitudinally applied magnetic field, we have $\mathbf{H}=H_x\mathbf{i}$ where $\mathbf{i}$ represents the unit vector associated with the x axis. Using Eqs. (1)–(3), the exerted forces per unit length of the ECS modeled based on the Rayleigh, Timoshenko, and higher-order beams, f_z^R, f_z^T, and f_z^H, respectively, are calculated as follows:

$$\begin{aligned}&f_z^R(x,t)=\varrho A_bH_x^2w^R_{,xx}(x,t),\\&f_z^T(x,t)=\varrho A_bH_x^2w^T_{,xx}(x,t),\\&f_z^H(x,t)=\varrho A_bH_x^2w^H_{,xx}(x,t),\end{aligned}\tag{4}$$

where A_b is the cross-section area of the ECS.

4. Wave propagation within a SWCNT under an axial steady magnetic field using NRBT

For an elastically confined SWCNT under a longitudinal magnetic field according to the NRBT, the governing equation in terms of the nonlocal bending moment, $(M_b^{nl})^R$, and the deflection of the ECS, w^R, is stated as

$$\rho_b(A_b\ddot{w}^R-I_b\ddot{w}^R_{,xx})-(M_b^{nl})^R_{,xx}+K_tw^R-K_rw^R_{,xx}=f_z^R,\tag{5}$$

where ρ_b and I_b are the density and the second moment inertia of the ECS pertinent to the SWCNT, respectively. According to the nonlocal continuum theory of Eringen [46,47], the nonlocal bending moment of the NRBT is expressed by

$$(M_b^{nl})^R-(e_0a)^2(M_b^{nl})^R_{,xx}=-E_bI_bw^R_{,xx},\tag{6}$$

in which a is an internal characteristic length, and e_0 is determined by adjusting the dispersion curves of the model with the reliably obtained results by experiments or other atomistic-based models. Substitution of the equivalent expression of $(M_b^{nl})^R_{,xx}$ from Eq. (5) into Eq. (6) leads to

$$\begin{aligned}(M_b^{nl})^R=&-E_bI_bw^R_{,xx}+(e_0a)^2(\rho_b(A_b\ddot{w}^R-I_b\ddot{w}^R_{,xx})-\varrho A_bH_x^2w^R_{,xx}\\&+K_tw^R-K_rw^R_{,xx}),\end{aligned}\tag{7}$$

substitution of Eq. (7) into Eq. (5) through using Eq. (4) yields the governing equation for the free transverse vibration of the NRB as follows:

$$\begin{aligned}&\rho_b(A_b\ddot{w}^R-I_b\ddot{w}^R_{,xx})-(e_0a)^2\rho_b(A_b\ddot{w}^R_{,xx}-I_b\ddot{w}^R_{,xxxx})\\&\quad+E_bI_bw^R_{,xxxx}-\varrho A_bH_x^2(w^R_{,xx}-(e_0a)^2w^R_{,xxxx})\\&\quad+K_t(w^R-(e_0a)^2w^R_{,xx})-K_r(w^R_{,xx}-(e_0a)^2w^R_{,xxxx})=0,\end{aligned}\tag{8}$$

Eq. (8) furnishes us with a mathematical model for free vibrating nanotube embedded in an elastic matrix under longitudinally induced magnetic field based on the NRBT. For more generalization of the problem analysis, the following dimensionless quantities are introduced:

$$\begin{aligned}&\xi=\frac{x}{l_b},\quad \overline{w}^R=\frac{w^R}{l_b},\quad \tau=\frac{1}{l_b^2}\sqrt{\frac{E_bI_b}{\rho_bA_b}}t,\quad \mu=\frac{e_0a}{l_b},\quad \lambda=\frac{l_b}{r_b},\\&\overline{K}_t^R=\frac{K_tl_b^4}{E_bI_b},\quad \overline{K}_r^R=\frac{K_rl_b^2}{E_bI_b},\quad \overline{H}_x^R=\sqrt{\frac{\varrho A_bl_b^2}{E_bI_b}}H_x,\end{aligned}\tag{9}$$

in which r_b denotes the gyration radius of the cross-section of the nanotube. Therefore, the dimensionless equation of motion of the nanotube structure modeled based on the NRBT are derived as

$$\begin{aligned}&\overline{w}^R_{,\tau\tau}-\mu^2\overline{w}^R_{,\tau\tau\xi\xi}-\lambda^{-2}(\overline{w}^R_{,\tau\tau\xi\xi}-\mu^2\overline{w}^R_{,\tau\tau\xi\xi\xi\xi})+\overline{w}^R_{,\xi\xi\xi\xi}\\&\quad-(\overline{H}_x^R)^2(\overline{w}^R_{,\xi\xi}-\mu^2\overline{w}^R_{,\xi\xi\xi\xi})+\overline{K}_t^R(\overline{w}^R-\mu^2\overline{w}^R_{,\xi\xi})\\&\quad-\overline{K}_r^R(\overline{w}^R_{,\xi\xi}-\mu^2\overline{w}^R_{,\xi\xi\xi\xi})=0.\end{aligned}\tag{10}$$

Let the transverse harmonic wave within the SWCNT could produce deflection $\overline{w}^R(\xi,\tau)=\overline{w}_0^R\,e^{i(\varpi^R\tau-\overline{k}\xi)}$ where $i=\sqrt{-1}$, τ is the dimensionless time parameter, $\overline{k}$ is the dimensionless wavenumber, $\overline{w}_0^R$ is the dimensionless amplitude deflection of the SWCNT, and ϖ^R denotes the dimensionless frequency of the transverse

propagated wave within the SWCNT modeled by the NRBT. By substituting this form of transverse displacement into Eq. (10), the dispersion relation could be expressed by

$$\varpi^R=\sqrt{\frac{\overline{k}^2((\overline{H}_x^R)^2+\overline{K}_r^R)+\overline{K}_t^R}{1+\lambda^{-2}\overline{k}^2}+\frac{\overline{k}^4}{(1+\mu^2\overline{k}^2)(1+\lambda^{-2}\overline{k}^2)}}. \tag{11}$$

The phase velocity of the wave is defined by $v_p^R=\omega^R/k$ where ω^R and k represent the frequency and wavenumber of the propagated wave, respectively. Therefore,

$$v_p^R=\sqrt{\frac{E_b}{\rho_b}\left(\frac{(\overline{H}_x^R)^2+\overline{K}_r^R+\overline{k}^{-2}\overline{K}_t^R}{\lambda^2+\overline{k}^2}+\frac{\overline{k}^2}{(1+\mu^2\overline{k}^2)(\lambda^2+\overline{k}^2)}\right)}, \tag{12}$$

and the group velocity of the wave is defined as $v_g^R=\partial\omega^R/\partial k$. Hence,

$$v_g^R=\frac{\overline{k}}{\lambda\varpi^R}\sqrt{\frac{E_b}{\rho_b}}\left(\frac{(\overline{H}_x^R)^2+\overline{K}_r^R-\lambda^{-2}\overline{K}_t^R}{(1+\lambda^{-2}\overline{k}^2)^2}+\frac{\overline{k}^2(2+(\mu^2+\lambda^{-2})\overline{k}^2)}{(1+\mu^2\overline{k}^2)^2(1+\lambda^{-2}\overline{k}^2)^2}\right). \tag{13}$$

The dimensionless cut-off frequency, ϖ_0^R, could be obtained from Eq. (11) by letting $\overline{k}=0$. So,

$$\varpi_0^R=\sqrt{\overline{K}_t^R} \tag{14}$$

as $k\to\infty$, the dimensionless asymptotic of the SWCNT subjected to the longitudinal magnetic field based on the NRBT, ϖ_a^R, is obtained as follows:

$$\varpi_a^R=\lambda\sqrt{(\overline{H}_x^R)^2+\overline{K}_r^R+\mu^{-2}}. \tag{15}$$

5. Wave propagation within a SWCNT under an axial steady magnetic field using NTBT

According to the NTBT, the governing equations in terms of nonlocal forces within the SWCNT as well as deformation fields of the ECS, embedded in an elastic matrix and subjected to a longitudinal magnetic field, are obtained as

$$\begin{aligned}&\rho_b I_b\ddot{\theta}^T-(Q_b^{nl})^T+(M_b^{nl})^T_{,x}+K_r\theta^T=0,\\&\rho_b A_b\ddot{w}^T-(Q_b^{nl})^T_{,x}+K_t w^T=f_z^T,\end{aligned} \tag{16}$$

where θ^T and $(Q_b^{nl})^T$ are the angle of deformation and resultant shear force of the NTB, respectively. Based on the nonlocal continuum theory of Eringen [46,47], the nonlocal forces within the NTB are defined as in the following form:

$$\begin{aligned}&(Q_b^{nl})^T-(e_0a)^2(Q_b^{nl})^T_{,xx}=k_sG_bA_b(w^T_{,x}-\theta^T),\\&(M_b^{nl})^T-(e_0a)^2(M_b^{nl})^T_{,xx}=-E_bI_b\theta^T_{,x},\end{aligned} \tag{17}$$

in which G_b is the shear modulus of elasticity defined by $G_b=E_b/(2(1+\nu))$ where ν is the Poisson's ratio of the material of the nanotube structure. The parameter k_s represents the shear correction factor of the cross-section of the single walled nanotube. By combining Eq. (16) with Eq. (17) through using Eq. (4), the nonlocal resultant shear force and bending moment within the NTB are obtained as

$$\begin{aligned}(Q_b^{nl})^T&=k_sG_bA_b(w^T_{,x}-\theta^T)+(e_0a)^2(\rho_bA_b\ddot{w}^T-\varrho A_bH_x^2w^T_{,xx}+K_tw^T)_{,x},\\(M_b^{nl})^T&=-E_bI_b\theta^T_{,x}+(e_0a)^2(\rho_bA_b\ddot{w}^T-\rho_bI_b\ddot{\theta}^T_{,x}-\varrho A_bH_x^2w^T_{,xx}\\&\quad+K_tw^T-K_r\theta^T_{,x}),\end{aligned} \tag{18}$$

substitution of Eq. (18) into Eq. (16) leads to

$$\begin{aligned}&\rho_bI_b(\ddot{\theta}^T-(e_0a)^2\ddot{\theta}^T_{,xx})-k_sG_bA_b(w^T_{,x}-\theta^T)-E_bI_b\theta^T_{,xx}+K_r(\theta^T-(e_0a)^2\theta^T_{,xx})=0,\\&\rho_bA_b(\ddot{w}^T-(e_0a)^2\ddot{w}^T_{,xx})-k_sG_bA_b(w^T_{,xx}-\theta^T_{,x})-\varrho A_bH_x^2(w^T_{,xx}-(e_0a)^2w^T_{,xxxx})\\&\quad+K_t(w^T-(e_0a)^2w^T_{,xx})=0,\end{aligned} \tag{19}$$

Eq. (19) represents the explicit expression of the governing equations in terms of deformation fields of the NTB. By introducing the following dimensionless parameters:

$$\begin{aligned}&\overline{w}^T=\frac{w^T}{l_b},\quad \overline{\theta}^T=\theta^T,\quad \tau=\frac{1}{l_b}\sqrt{\frac{k_sG_b}{\rho_b}}t,\quad \eta=\frac{E_bI_b}{k_sG_bA_bl_b^2},\\&\overline{K}_r^T=\frac{K_r}{k_sG_bA_b},\quad \overline{K}_t^T=\frac{K_tl_b^2}{k_sG_bA_b},\quad \overline{H}_x^T=\sqrt{\frac{\varrho}{k_sG_b}}H_x,\end{aligned} \tag{20}$$

Eq. (19) is rewritten in the nondimensional form as follows:

$$\begin{aligned}&\lambda^{-2}(\overline{\theta}^T_{,\tau\tau}-\mu^2\overline{\theta}^T_{,\tau\tau\xi\xi})-\overline{w}^T_{,\xi}+\overline{\theta}^T-\eta\overline{\theta}^T_{,\xi\xi}+\overline{K}_r^T(\overline{\theta}^T-\mu^2\overline{\theta}^T_{,\xi\xi})=0,\\&\overline{w}^T_{,\tau\tau}-\mu^2\overline{w}^T_{,\tau\tau\xi\xi}-\overline{w}^T_{,\xi\xi}+\overline{\theta}^T_{,\xi}-(\overline{H}_x^T)^2(\overline{w}^T_{,\xi\xi}-\mu^2\overline{w}^T_{,\xi\xi\xi\xi})\\&\quad+\overline{K}_t^T(\overline{w}^T-\mu^2\overline{w}^T_{,\xi\xi})=0.\end{aligned} \tag{21}$$

The harmonic solution of the propagated waves within the SWCNT experiences longitudinal magnetic field and is modeled based on the NTBT, could be considered as $\overline{\theta}^T(\xi,\tau)=\overline{\theta}_0^Te^{i(\varpi^T\tau-\overline{k}\xi)}$ and $\overline{w}^T(\xi,\tau)=\overline{w}_0^Te^{i(\varpi^T\tau-\overline{k}\xi)}$ where $\overline{\theta}_0^T$ and $\overline{w}_0^T$ denote the amplitude of harmonic waves pertinent to the deflection angle and deflection of the SWCNT, respectively. Substituting such expressions into the dimensionless form of the governing equations, Eq. (21), the following set of algebraic equations is obtained:

$$\begin{bmatrix}C_1^T & C_2^T\\ C_3^T & C_4^T\end{bmatrix}\begin{Bmatrix}\overline{\theta}_0^T\\ \overline{w}_0^T\end{Bmatrix}=\begin{Bmatrix}0\\0\end{Bmatrix}, \tag{22}$$

where the elements of the coefficient matrix are as follows:

$$\begin{aligned}&C_1^T=-(\varpi^T)^2\lambda^{-2}(1+\mu^2\overline{k}^2)+1+\eta\overline{k}^2+\overline{K}_r^T(1+\mu^2\overline{k}^2),\\&C_2^T=i\overline{k},C_3^T=-i\overline{k},\\&C_4^T=-(\varpi^T)^2(1+\mu^2\overline{k}^2)+\overline{k}^2+((\overline{H}_x^T)^2\overline{k}^2+\overline{K}_t^T)(1+\mu^2\overline{k}^2),\end{aligned} \tag{23}$$

there exists a nontrivial solution to the set of equations in Eq. (22) if and only if the determinant of the coefficient matrix is set equal to zero. Therefore, the following characteristic equation (i.e., dispersion relation) is obtained:

$$\begin{aligned}&(\varpi^T)^4\lambda^{-2}(1+\mu^2\overline{k}^2)^2-(\varpi^T)^2(1+\mu^2\overline{k}^2)(1+\eta\overline{k}^2+\overline{K}_r^T(1+\mu^2\overline{k}^2)\\&\quad+\lambda^{-2}(\overline{k}^2+((\overline{H}_x^T)^2\overline{k}^2+\overline{K}_t^T)\quad+(1+\eta\overline{k}^2+\overline{K}_r^T(1+\mu^2\overline{k}^2))\\&(\overline{k}^2+((\overline{H}_x^T)^2\overline{k}^2+\overline{K}_t^T)\quad(1+\mu^2\overline{k}^2))-\overline{k}^2=0.\end{aligned} \tag{24}$$

Eq. (24) is a second-order algebraic equation for $(\varpi^T)^2$. Therefore, there would be two wave modes for the transverse vibration of SWCNT under a longitudinal magnetic field based on the NTBT. The dimensionless frequencies of the wave modes are readily calculated as

$$\begin{aligned}\varpi_1^T&=\sqrt{\frac{\alpha_2^2+\lambda^{-2}\alpha_3^2-\sqrt{(\alpha_2^2-\lambda^{-2}\alpha_3^2)^2+4\lambda^{-2}\overline{k}^2}}{2\alpha_1^2}},\\\varpi_2^T&=\sqrt{\frac{\alpha_2^2+\lambda^{-2}\alpha_3^2+\sqrt{(\alpha_2^2-\lambda^{-2}\alpha_3^2)^2+4\lambda^{-2}\overline{k}^2}}{2\alpha_1^2}},\end{aligned} \tag{25}$$

where $\alpha_i^2;i=1,2,3$ are as

$$\begin{aligned}&\alpha_1^2=\lambda^{-2}(1+\mu^2\overline{k}^2),\quad \alpha_2^2=1+\eta\overline{k}^2+\overline{K}_r^T(1+\mu^2\overline{k}^2),\\&\alpha_3^2=k^2+(1+\mu^2\overline{k}^2)(\overline{K}_t^T+\overline{k}^2(\overline{H}_x^T)^2),\end{aligned} \tag{26}$$

and the phase velocities of the propagated sound waves, $v_{pi}^T=\omega_i^T/k$, are determined as

$$v_{p1}^T=\sqrt{\frac{k_sG_b}{\rho_b}\left(\frac{\alpha_2^2+\lambda^{-2}\alpha_3^2-\sqrt{(\alpha_2^2-\lambda^{-2}\alpha_3^2)^2+4\lambda^{-2}\overline{k}^2}}{2\overline{k}^2\alpha_1^2}\right)},$$
$$v_{p2}^T=\sqrt{\frac{k_sG_b}{\rho_b}\left(\frac{\alpha_2^2+\lambda^{-2}\alpha_3^2+\sqrt{(\alpha_2^2-\lambda^{-2}\alpha_3^2)^2+4\lambda^{-2}\overline{k}^2}}{2\overline{k}^2\alpha_1^2}\right)}, \tag{27}$$

where ω_i^T denotes the frequency of the sound wave propagated within the SWCNT subjected to an axial magnetic field and modeled based on the NTBT. It should be noted that the wave modes with lower levels of frequencies and phase velocities are pertinent to flexural waves, while the wave modes with higher levels of frequencies and phase velocities are pertinent to shear waves [51].

The group velocities of the propagated sound waves within the SWCNT under uniaxial magnetic field based on the NTBT are evaluated by $v_{gi}^T=\partial\omega_i^T/\partial k$. Hence, the group velocities associated with the flexural and shear waves, respectively, denoted by v_{g1}^T and v_{g2}^T, are determined as

$$v_{g1}^T=\sqrt{\frac{k_sG_b}{\rho_b}}\left(\frac{\left(\begin{array}{l}\alpha_2\alpha_{2,\overline{k}}+2\lambda^{-2}\alpha_3\alpha_{3,\overline{k}}-2((\alpha_2\alpha_{2,\overline{k}}-\lambda^{-2}\alpha_3\alpha_{3,\overline{k}})\\ \times(\alpha_2^2-\lambda^{-2}\alpha_3^2)+2\lambda^{-2}\overline{k})((\alpha_2^2-\lambda^{-2}\alpha_3^2)^2+4\lambda^{-2}\overline{k}^2)^{-1/2}\end{array}\right)}{\alpha_1^2\varpi_1^T}-\frac{\alpha_{1,\overline{k}}\varpi_1^T}{\alpha_1^2}\right),$$
$$v_{g2}^T=\sqrt{\frac{k_sG_b}{\rho_b}}\left(\frac{\left(\begin{array}{l}\alpha_2\alpha_{2,\overline{k}}+2\lambda^{-2}\alpha_3\alpha_{3,\overline{k}}+2((\alpha_2\alpha_{2,\overline{k}}-\lambda^{-2}\alpha_3\alpha_{3,\overline{k}})\\ \times(\alpha_2^2-\lambda^{-2}\alpha_3^2)+2\lambda^{-2}\overline{k})((\alpha_2^2-\lambda^{-2}\alpha_3^2)^2+4\lambda^{-2}\overline{k}^2)^{-1/2}\end{array}\right)}{\alpha_1^2\varpi_2^T}-\frac{\alpha_{1,\overline{k}}\varpi_2^T}{\alpha_1^2}\right), \tag{28}$$

where $\alpha_{1,\overline{k}}$ $\alpha_{2,\overline{k}}$, and $\alpha_{3,\overline{k}}$ represent the first derivative of α_1, α_2, and α_3 with respect to $\overline{k}$, respectively. By letting $k=0$ in Eq. (27), the dimensionless cut-off frequencies of flexural and shear waves, represented by ϖ_{10}^T and ϖ_{20}^T, respectively, are obtained as

$$\varpi_{10}^T=\begin{cases}\lambda\sqrt{1+\overline{K}_r^T}; & \overline{K}_t^T>\lambda^2(1+\overline{K}_r^T)\\ \sqrt{\overline{K}_t^T}; & \overline{K}_t^T<\lambda^2(1+\overline{K}_r^T)\end{cases}, \tag{29}$$

and

$$\varpi_{20}^T=\begin{cases}\sqrt{\overline{K}_t^T}; & \overline{K}_t^T>\lambda^2(1+\overline{K}_r^T)\\ \lambda\sqrt{1+\overline{K}_r^T}; & \overline{K}_t^T<\lambda^2(1+\overline{K}_r^T)\end{cases}, \tag{30}$$

and in limit when k goes to infinity, the dimensionless asymptotic frequencies of the flexural and shear waves, denoted by ϖ_{1a}^T and ϖ_{2a}^T, respectively, could be determined from

$$\varpi_{10}^T=\begin{cases}\overline{H}_x^T; & \eta+\mu^2\overline{K}_r^T>\mu^2\lambda^{-2}(\overline{H}_x^T)^2\\ \frac{\lambda}{\mu}\sqrt{\eta+\mu^2\overline{K}_r^T}; & \eta+\mu^2\overline{K}_r^T<\mu^2\lambda^{-2}(\overline{H}_x^T)^2\end{cases} \tag{31}$$

and

$$\varpi_{20}^T=\begin{cases}\frac{\lambda}{\mu}\sqrt{\eta+\mu^2\overline{K}_r^T}; & \eta+\mu^2\overline{K}_r^T>\mu^2\lambda^{-2}(\overline{H}_x^T)^2\\ \overline{H}_x^T; & \eta+\mu^2\overline{K}_r^T<\mu^2\lambda^{-2}(\overline{H}_x^T)^2\end{cases}. \tag{32}$$

6. Wave propagation within a SWCNT under an axial steady magnetic field using NHOBT

According to the NHOBT, the governing equations in terms of nonlocal forces and deformation fields for a nanotube embedded in an elastic medium are expressed as

$$(I_2-2\alpha I_4+\alpha^2I_6)\ddot{\psi}^H+(\alpha^2I_6-\alpha I_4)\ddot{w}_{,x}^H+(Q_b^{nl})^H+\alpha(P_b^{nl})_{,x}^H-(M_b^{nl})_{,x}^H+K_r\psi^H=0,$$
$$I_0\ddot{w}^H-(\alpha^2I_6-\alpha I_4)\ddot{\psi}_{,x}^H-\alpha^2I_6\ddot{w}_{,xx}^H-(Q_b^{nl})_{,x}^H-\alpha(P_b^{nl})_{,xx}^H+K_tw^H=f_z^H, \tag{33}$$

where ψ^H denotes the deflection angle of the NHOB. According to the nonlocal continuum theory of Eringen, the nonlocal forces within the NHOB are stated as

$$(M_b^{nl})^H-(e_0a)^2(M_b^{nl})_{,xx}^H=J_2\psi_{,x}^H-\alpha J_4(\psi_{,x}^H+w_{,xx}^H),$$
$$(Q_b^{nl}+\alpha P_{b,x}^{nl})^H-(e_0a)^2(Q_b^{nl}+\alpha P_{b,x}^{nl})_{,xx}^H=\kappa(\psi^H+w_{,x}^H)+\alpha J_4\psi_{,xx}^H-\alpha^2J_6(\psi_{,xx}^H+w_{,xxx}^H), \tag{34}$$

where

$$\kappa=\int_{A_b}G_b(1-3\alpha z^2)\,dA,\quad I_n=\int_{A_b}\rho_bz^n\,dA,\quad J_n=\int_{A_b}E_bz^n\,dA, \tag{35}$$

where $\alpha=4/(3D_o^2)$ and D_o denotes the outer diameter of the ECS. By substitution of the equivalent values of $(M_b^{nl})^H$ and $(Q_b^{nl}+\alpha P_{b,x}^{nl})^H$ from Eq. (33) into Eq. (34), one arrives at

$$\begin{aligned}(M_b^{nl})^H&=J_2\psi_{,x}^H-\alpha J_4(\psi_{,x}^H+w_{,xx}^H)+(e_0a)^2((I_2-\alpha I_4)\ddot{\psi}_{,x}^H+I_0\ddot{w}^H\\&\quad-\alpha I_4\ddot{w}_{,xx}^H-\varrho A_bH_x^2w_{,xx}^H+K_tw^H+K_r\psi_{,x}^H),\\(Q_b^{nl}+\alpha P_{b,x}^{nl})^H&=\kappa(\psi^H+w_{,x}^H)+\alpha J_4\psi_{,xx}^H-\alpha^2J_6(\psi_{,xx}^H+w_{,xxx}^H)\\&\quad+(e_0a)^2(I_0\ddot{w}_{,x}^H-\varrho A_bH_x^2w_{,xxx}^H+K_tw_{,x}^H-(\alpha^2I_6-\alpha I_4)\ddot{\psi}_{,xx}^H\\&\quad-\alpha^2I_6\ddot{w}_{,xxxx}^H),\end{aligned} \tag{36}$$

substitution of Eq. (36) into Eq. (33) through using Eq. (4) leads to the nonlocal equations of motion in terms of displacements as in the following form:

$$\begin{aligned}&(I_2-2\alpha I_4+\alpha^2I_6)(\ddot{\psi}^H-(e_0a)^2\ddot{\psi}_{,xx}^H)+(\alpha^2I_6-\alpha I_4)(\ddot{w}_{,x}^H-(e_0a)^2\ddot{w}_{,xxx}^H)\\&\quad+\kappa(\psi^H+w_{,x}^H)-(J_2-2\alpha J_4+\alpha^2J_6)\psi_{,xx}^H+(\alpha J_4-\alpha^2J_6)w_{,xxx}^H\\&\quad+K_r(\psi^H-(e_0a)^2\psi_{,xx}^H)=0,\\&I_0(\ddot{w}^H-(e_0a)^2\ddot{w}_{,xx}^H)-(\alpha^2I_6-\alpha I_4)(\ddot{\psi}_{,x}^H-(e_0a)^2\ddot{\psi}_{,xxx}^H)\\&\quad-\alpha^2I_6(\ddot{w}_{,xx}^H-(e_0a)^2\ddot{w}_{,xxxx}^H)\\&\quad-\kappa(\psi_{,x}^H+w_{,xx}^H)-\alpha J_4\psi_{,xxx}^H+\alpha^2J_6(\psi_{,xx}^H+w_{,xxx}^H)\\&\quad-\varrho A_bH_x^2(w_{,xx}^H-(e_0a)^2w_{,xxxx}^H)+K_t(w^H-(e_0a)^2w_{,xx}^H)=0,\end{aligned} \tag{37}$$

Eq. (37) shows the incorporation of the small scale parameter into the governing equations of an elastically supported NHOB embedded in an elastic matrix. By introducing the following dimensionless quantities:

$$\overline{w}^H=\frac{w^H}{l_b},\quad\overline{\psi}^H=\psi^H,\quad\tau=\frac{\alpha}{l_b^2}\sqrt{\frac{J_6}{I_0}}t,\quad\gamma_1^2=\frac{\alpha I_4-\alpha^2I_6}{I_0l_b^2},$$
$$\gamma_2^2=\frac{\alpha^2I_6}{I_0l_b^2},\quad\gamma_3^2=\frac{\kappa l_b^2}{\alpha^2J_6},\quad\gamma_4^2=\frac{\alpha J_4-\alpha^2J_6}{\alpha^2J_6},$$
$$\gamma_6^2=\frac{\alpha I_4-\alpha^2I_6}{I_2-2\alpha I_4+\alpha^2I_6},\quad\gamma_7^2=\frac{\kappa I_0l_b^4}{(I_2-2\alpha I_4+\alpha^2I_6)\alpha^2J_6},$$
$$\gamma_8^2=\frac{(J_2-2\alpha J_4+\alpha^2J_6)I_0l_b^2}{(I_2-2\alpha I_4+\alpha^2I_6)\alpha^2J_6},\quad\gamma_9^2=\frac{(\alpha J_4-\alpha^2J_6)I_0l_b^2}{(I_2-2\alpha I_4+\alpha^2I_6)\alpha^2J_6},$$
$$\overline{K}_r^H=\frac{K_rI_0l_b^4}{\alpha^2(I_2-2\alpha I_4+\alpha^2I_6)J_6},\quad\overline{K}_t^H=\frac{K_tl_b^4}{\alpha^2J_6},\quad\overline{H}_x^H=\sqrt{\frac{\varrho A_bl_b^2}{\alpha^2J_6}}H_x, \tag{38}$$

the dimensionless equations of motion of the SWCNT subjected to a longitudinal magnetic field on the basis of the NHOBT are obtained as follows:

$$\begin{aligned}&\overline{\psi}_{,\tau\tau}^H-\mu^2\overline{\psi}_{,\xi\xi\tau\tau}^H-\gamma_6^2(\overline{w}_{,\tau\tau\xi}^H-\mu^2\overline{w}_{,\tau\tau\xi\xi\xi}^H)+\gamma_7^2(\overline{\psi}^H+\overline{w}_{,\xi}^H)\\&\quad-\gamma_8^2\overline{\psi}_{,\xi\xi}^H+\gamma_9^2\overline{w}_{,\xi\xi\xi}^H+\overline{K}_r^H(\overline{\psi}^H-\mu^2\overline{\psi}_{,\xi\xi}^H)=0,\end{aligned}$$

$$\overline{w}^H_{,\tau\tau}-\mu^2\overline{w}^H_{,\tau\tau\xi\xi}+\gamma_1^2(\overline{\psi}^H_{,\tau\tau\xi}-\mu^2\overline{\psi}^H_{,\tau\tau\xi\xi\xi})-\gamma_2^2(\overline{w}^H_{,\tau\tau\xi\xi}-\mu^2\overline{w}^H_{,\tau\tau\xi\xi\xi\xi})$$
$$-\gamma_3^2(\overline{\psi}^H_{,\xi}+\overline{w}^H_{,\xi\xi})-\gamma_4^2\overline{\psi}^H_{,\xi\xi\xi}+\overline{w}^H_{,\xi\xi\xi\xi}-(\overline{H}^H_x)^2(\overline{w}^H_{,\xi\xi}-\mu^2\overline{w}^H_{,\xi\xi\xi\xi})$$
$$+\overline{K}^H_t(\overline{w}^H-\mu^2\overline{w}^H_{,\xi\xi})=0. \tag{39}$$

A harmonic solution to the coupled equations in Eq. (39) could be considered as $\overline{\psi}^H(\xi,\tau)=\overline{\psi}^H_0 e^{i(\varpi^H\tau-\overline{k}\xi)}$ and $\overline{w}^H(\xi,\tau)=\overline{w}^H_0 e^{i(\varpi^H\tau-\overline{k}\xi)}$ where $\overline{\psi}^H_0$ and $\overline{w}^H_0$ are the amplitude of harmonic waves pertinent to the deflection angle and deflection of the SWCNT modeled based on the NHOBT, respectively. By substituting such a solution into the governing equations, Eq. (39), the following set of algebraic equations is obtained:

$$\begin{bmatrix} C^H_1 & C^H_2 \\ C^H_3 & C^H_4 \end{bmatrix}\begin{Bmatrix} \overline{\psi}^H_0 \\ \overline{w}^H_0 \end{Bmatrix}=\begin{Bmatrix} 0 \\ 0 \end{Bmatrix}, \tag{40}$$

where the elements of the coefficient matrix are as follows:

$$C^H_1=-(\varpi^H)^2(1+\mu^2\overline{k}^2)+\gamma_7^2+\overline{k}^2\gamma_8^2+\overline{K}^H_r(1+\mu^2\overline{k}^2),$$
$$C^H_2=-i\overline{k}((\varpi^H)^2(1+\mu^2\overline{k}^2)\gamma_6^2+\gamma_7^2-\overline{k}^2\gamma_9^2),$$
$$C^H_3=i\overline{k}((\varpi^H)^2(1+\mu^2\overline{k}^2)\gamma_1^2+\gamma_3^2-\overline{k}^2\gamma_4^2),$$
$$C^H_4=-(\varpi^H)^2(1+\mu^2\overline{k}^2)(1+\gamma_2^2\overline{k}^2)+\gamma_3^2\overline{k}^2+\overline{k}^4+(1+\overline{k}^2(\overline{H}^H_x))(1+\mu^2\overline{k}^2), \tag{41}$$

In Eq. (40), by setting the determinant of the coefficient matrix equal to zero, the dispersion relation of the propagated sound waves within the SWCNT modeled in accordance with the hypotheses of the NHOBT, is derived as follows:

$$A^H(\overline{k})(\varpi^H)^4+B^H(\overline{k})(\varpi^H)^2+C^H(\overline{k})=0, \tag{42}$$

where

$$A^H(\overline{k})=(1+\mu^2\overline{k}^2)^2(1+(\gamma_2^2+\gamma_1^2\gamma_6^2)\overline{k}^2),$$
$$B^H(\overline{k})=(1+\mu^2\overline{k}^2)\begin{pmatrix}\gamma_3^2\overline{k}^2+\overline{k}^4+(\overline{K}^H_t+\overline{k}^2(\overline{H}^H_x)^2)(1+\mu^2\overline{k}^2)\\ +(1+\gamma_2^2\overline{k}^2)(\gamma_7^2+\gamma_8^2\overline{k}^2+\overline{K}^H_r(1+\mu^2\overline{k}^2))\\ +\overline{k}^2(\gamma_6^2(\gamma_3^2-\gamma_4^2\overline{k}^2)+\gamma_1^2(\gamma_7^2-\gamma_9^2\overline{k}^2))\end{pmatrix},$$
$$C^H(\overline{k})=(\gamma_7^2+\gamma_8^2\overline{k}^2+\overline{K}^H_r(1+\mu^2\overline{k}^2))(\gamma_3^2\overline{k}^2+\overline{k}^4$$
$$+(\overline{K}^H_t+\overline{k}^2(\overline{H}^H_x)^2)(1+\mu^2\overline{k}^2))-\overline{k}^2(\gamma_7^2-\gamma_9^2\overline{k}^2)(\gamma_3^2-\gamma_4^2\overline{k}^2). \tag{43}$$

Eq. (42) is a second-order algebraic equation for $(\varpi^H)^2$. Therefore, the dimensionless frequencies pertinent to the flexural and shear waves are easily calculated as

$$\varpi^H_1=\sqrt{\frac{B^H-\sqrt{(B^H)^2-4A^HC^H}}{2A^H}},$$
$$\varpi^H_2=\sqrt{\frac{B^H+\sqrt{(B^H)^2-4A^HC^H}}{2A^H}}, \tag{44}$$

and the phase velocities of the propagated sound waves, $\nu^H_{pi}=\omega^H_i/k$; $i=1,2$, are obtained as

$$\nu^H_{p1}=\frac{\alpha}{l_b}\sqrt{\frac{J_6}{I_0}\left(\frac{B^H-\sqrt{(B^H)^2-4A^HC^H}}{2A^H}\right)},$$
$$\nu^H_{p2}=\frac{\alpha}{l_b}\sqrt{\frac{J_6}{I_0}\left(\frac{B^H+\sqrt{(B^H)^2-4A^HC^H}}{2A^H}\right)}, \tag{45}$$

where ω^H_i denotes the frequency of the sound wave propagated within the SWCNT subjected to an axial magnetic field and modeled based on the NHOBT. The group velocities are also evaluated by $\nu^H_{gi}=\partial\omega^H_i/\partial k; i=1,2$. Hence,

$$\nu^H_{g1}=\frac{\alpha}{l_b}\sqrt{\frac{J_6}{I_0}}\left(\frac{B^H_{,\overline{k}}-((B^H)^2-4A^HC^H)^{-1/2}(B^HB^H_{,\overline{k}}-2(A^H_{,\overline{k}}C^H+A^HC^H_{,\overline{k}}))}{2A^H\varpi^H_1}-\frac{A^H_{,\overline{k}}\varpi^H_1}{A^H}\right),$$
$$\nu^H_{g2}=\frac{\alpha}{l_b}\sqrt{\frac{J_6}{I_0}}\left(\frac{B^H_{,\overline{k}}+((B^H)^2-4A^HC^H)^{-1/2}(B^HB^H_{,\overline{k}}-2(A^H_{,\overline{k}}C^H+A^HC^H_{,\overline{k}}))}{2A^H\varpi^H_2}-\frac{A^H_{,\overline{k}}\varpi^H_2}{A^H}\right), \tag{46}$$

where $A^H_{,\overline{k}}$, $B^H_{,\overline{k}}$, and $C^H_{,\overline{k}}$ represent the first derivative of functions $A^H(\overline{k})$, $B^H(\overline{k})$, and $C^H(\overline{k})$ with respect to $\overline{k}$, respectively. By letting $\overline{k}=0$ in Eq. (44), the dimensionless cut-off frequencies of flexural and shear waves, respectively, denoted by ϖ^H_{10} and ϖ^H_{20}, are obtained as

$$\varpi^H_{10}=\begin{cases}\sqrt{\gamma_7^2+\overline{K}^H_r}; & \overline{K}^H_t>\overline{K}^H_r+\gamma_7^2\\ \sqrt{\overline{K}^H_t}; & \overline{K}^H_t<\overline{K}^H_r+\gamma_7^2\end{cases}, \tag{47}$$

and

$$\varpi^H_{20}=\begin{cases}\sqrt{\overline{K}^H_t}; & \overline{K}^H_t>\overline{K}^H_r+\gamma_7^2\\ \sqrt{\gamma_7^2+\overline{K}^H_r}; & \overline{K}^H_t<\overline{K}^H_r+\gamma_7^2\end{cases}. \tag{48}$$

Moreover, the dimensionless asymptotic frequencies of the flexural and shear waves could be determined from Eq. (44) as $k\to\infty$. Therefore,

$$\varpi^H_{1a}=\sqrt{\frac{2\tilde{C}^H}{\tilde{B}^H+\sqrt{(\tilde{B}^H)^2-4\tilde{A}^H\tilde{C}^H}}},$$
$$\varpi^H_{2a}=\sqrt{\frac{2\tilde{C}^H}{\tilde{B}^H-\sqrt{(\tilde{B}^H)^2-4\tilde{A}^H\tilde{C}^H}}}, \tag{49}$$

where

$$\tilde{A}^H=\mu^4(\gamma_2^2+\gamma_1^2\gamma_6^2),$$
$$\tilde{B}^H=\mu^2(1+\mu^2((\overline{H}^H_x)^2+\gamma_2^2\overline{K}^H_r)+\gamma_2^2\gamma_8^2-\gamma_4^2\gamma_6^2+\gamma_1^2\gamma_9^2),$$
$$\tilde{C}^H=(1+\mu^2(\overline{H}^H_x)^2)(\gamma_8^2+\mu^2\overline{K}^H_r)-\gamma_4^2\gamma_9^2. \tag{50}$$

7. Results and discussions

In this section, the effect of slenderness ratio, mean radius of the ECS, axial magnetic field, small-scale parameter, and the elastic stiffness of the surrounding medium of the SWCNT on the frequencies, phase velocities, and group velocities of the transverse waves is investigated using the proposed models. For this purpose, consider an ECS pertinent to a SWCNT with the following data: $E_b=1$ TPa, $\nu=0.2$, $\rho_b=2500$ kg/m^3, $l_b=30$ nm, $r_m=2.5$ nm, and $t_b=0.34$ nm. In all plotted results, the predicted results by the NRBT, NTBT, and NHOBT are shown by the dotted, dashed, and solid lines, respectively. Further, the results associated with the flexural waves are identified by empty markers whereas those results pertinent to the shear waves are denoted by the filled markers.

In Fig. 2, the predicted results by the proposed nonlocal beam models as a function of the slenderness ratio are provided for different levels of the longitudinally applied magnetic field. The results are provided in the case of a SWCNT with $e_0a=2$ nm which has been released from the surrounding elastic medium (i.e., $K_r=K_t=0$). As it is seen in Fig. 2, the predicted flexural frequencies and the corresponding phase velocities of various beam models generally increase with the longitudinal magnetic field. This matter is more obvious for SWCNTs with low levels of

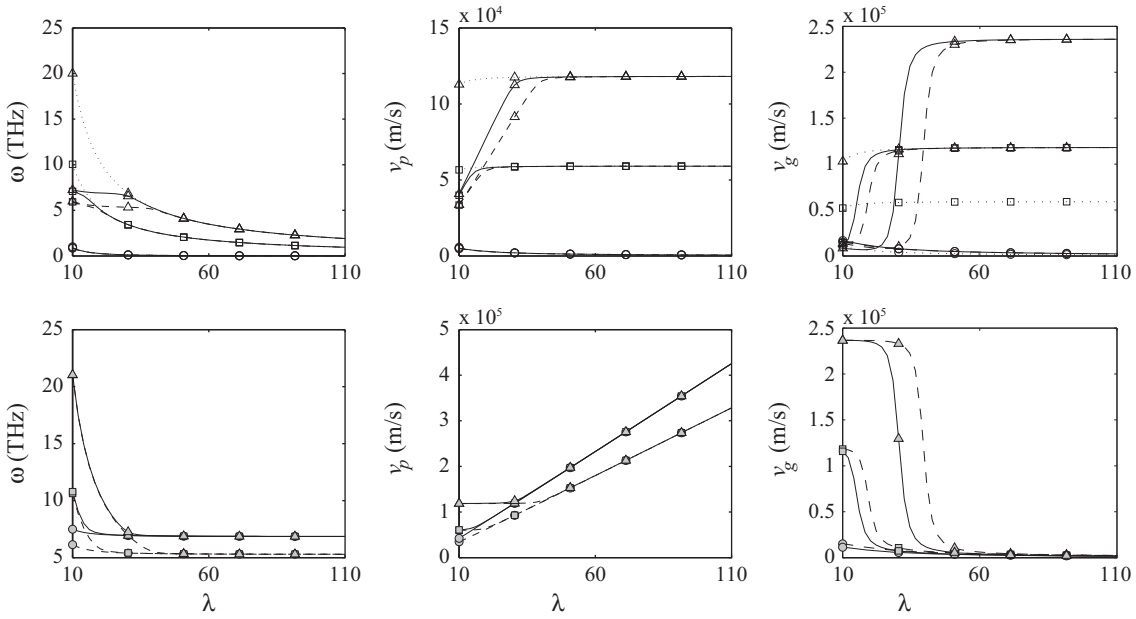

Fig. 2. Variation of frequencies, phase velocities, and group velocities corresponding to $\overline{k}=\pi$ in terms of slenderness ratio for different levels of axial magnetic field ((○) $\overline{H}_x^R=0$, (□) $\overline{H}_x^R=50$, (△) $\overline{H}_x^R=100$; (...) NRBT, (− · −) NTBT, (—) NHOBT; $e_0a=2$ nm; $K_r=K_t=0$).

the slenderness ratio. In such stocky nanostructures, the discrepancies between the results of the NRBT and the nonlocal shear deformable beam models are apparent, particularly for high levels of the longitudinal magnetic field. For most values of the slenderness ratio, the flexural frequencies and the corresponding phase velocities of the NHOBT are between the results of the NRBT and those of the NTBT. For low levels of the slenderness ratio, the shear frequencies and the related phase velocities of the NTBT and the NHOBT are fairly in line and close to each other for different levels of the longitudinal magnetic field. For a slenderness ratio greater than a certain value, variation of the slenderness ratio has a trivial effect on the variation of the shear frequencies of both the NTBT and the NHOBT. In the case of $\overline{H}_x=0$, there is a linear relationship between the phase velocities of the nonlocal shear deformable beams and the slenderness ratio. For $\overline{H}_x>0$, for a slenderness ratio greater than a certain value, the phase velocity would linearly vary in terms of the slenderness ratio of the SWCNT. In the case of $\overline{k}=\pi$, the group velocities pertinent to the shear waves decrease with the slenderness ratio, irrespective of the assumed level of the longitudinal magnetic field. However, it is not the case for those associated with the flexural waves. Regardless of $\overline{H}_x=0$, the group velocities of flexural waves of various beam models generally magnify as the slenderness ratio of the SWCNT increases.

The effect of the mean radius of the ECS on the frequencies as well as the corresponding phase and group velocities of the shear and flexural waves is studied for different levels of the longitudinal magnetic field. The length of the SWCNT is considered to be constant and only its mean radius varies. The predicted results by various nonlocal beam models for the wavenumber of the first vibration mode (i.e., $\overline{k}=\pi$) as a function of normalized mean radius are presented in Fig. 3. As it is obvious in Fig. 3, the differences between the flexural frequencies of the NRBT and those of the nonlocal shear deformable beam models commonly increase as the radius of the SWCNT increases. This matter is also valid for the phase velocities of the flexural waves. Such discrepancies are more obvious for higher levels of the longitudinally applied magnetic field. In the case of $\overline{H}_x=0$, the predicted flexural frequencies by various nonlocal beams increase with the radius of the SWCNT. However, in the cases of $\overline{H}_x=50$ as well as $\overline{H}_x=100$, the flexural frequencies of the proposed nonlocal beams decrease with the radius of the SWCNT. Regarding shear wave modes, the predicted shear frequencies of the NTBT and the NHOBT generally decrease with the radius of the SWCNT. The rate of variation of shear frequency as a function of radius of the SWCNT is more apparent in the case of $\overline{H}_x=0$ with respect to other cases. For both flexural and shear waves, the discrepancies between the frequencies (or even the corresponding phase and group velocities) of the NTBT and those of the NHOBT generally decrease with the mean radius of the ECS.

Another interesting study is carried out to determine the effect of longitudinal magnetic field on the dispersion curves, phase and group velocities of the propagated transverse waves within the SWCNT. In Fig. 4, the predicted results by the proposed models are presented for three levels of the axially applied magnetic field (i.e., $\overline{H}_x=$ 0, 5, and 10) for a SWCNT with $\lambda=15$ and $e_0a=2$ nm. As it is seen in Fig. 4, for most of the wavenumbers, the predicted flexural frequencies as well as the corresponding phase velocities by the NHOBT are between the predicted results by the NRBT and those of the NTBT. Generally, the discrepancies between the results of the NRBT and those of the nonlocal shear deformable beam models increase with the wavenumber, irrespective of the applied longitudinal magnetic field. Further, the differences between the dispersion curves of the NHOBT which are pertinent to the shear wave modes and those of the NTBT increase with the wavenumber. This matter is more apparent for higher levels of the longitudinally applied magnetic field. The predicted flexural group velocities by the NTBT and those of the NHOBT are generally in line. However, the shear group velocities by the NTBT and those of the NHOBT are in line for low levels of the wavenumbers. As the applied longitudinal magnetic field increases, the discrepancies between the shear group velocities of the NTBT and those of the NHOBT commonly amplify, particularly for higher levels of the wavenumber.

In another detailed scrutiny, the influence of the applied longitudinal magnetic field on the frequencies, phase and group velocities of the propagated waves within the SWCNT are of particular interest for different levels of the wavenumber. In doing so, the plotted results of the NRBT, NTBT, and NHOBT are provided in Fig. 5 for three values of the dimensionless

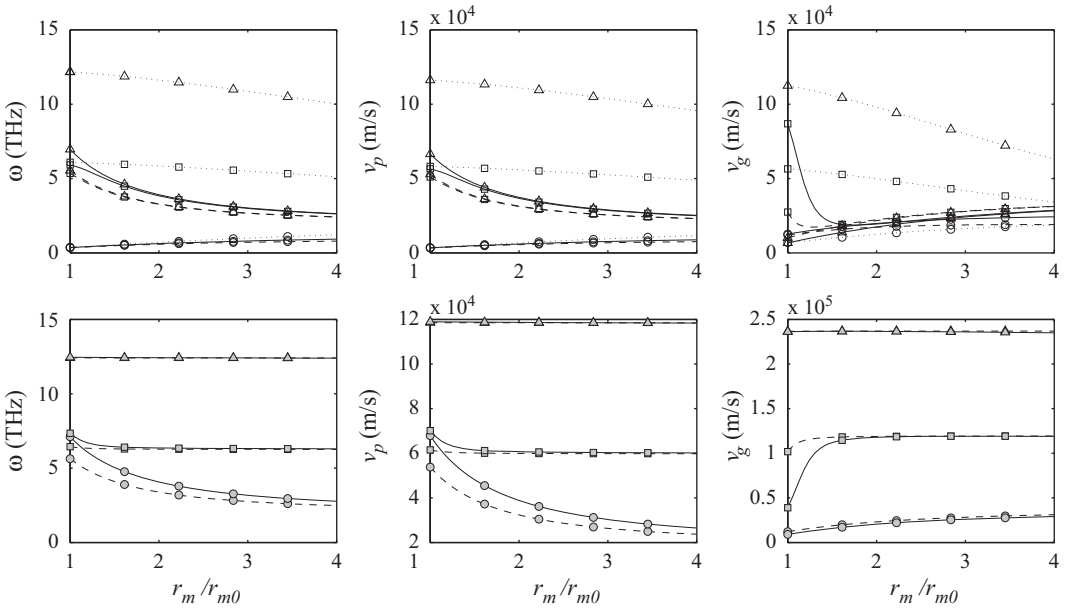

Fig. 3. Variation of frequencies, phase velocities, and group velocities corresponding to $\overline{k}=\pi$ in terms of normalized mean radius of the SWCNT for different levels of axial magnetic field ((○) $\overline{H}_x^R=0$, (□) $\overline{H}_x^R=50$, (△) $\overline{H}_x^R=100$; (...) NRBT, (– · –) NTBT, (—) NHOBT; $e_0a=2$ nm, $r_{m0}=2.5$ nm, $K_r=K_t=0$).

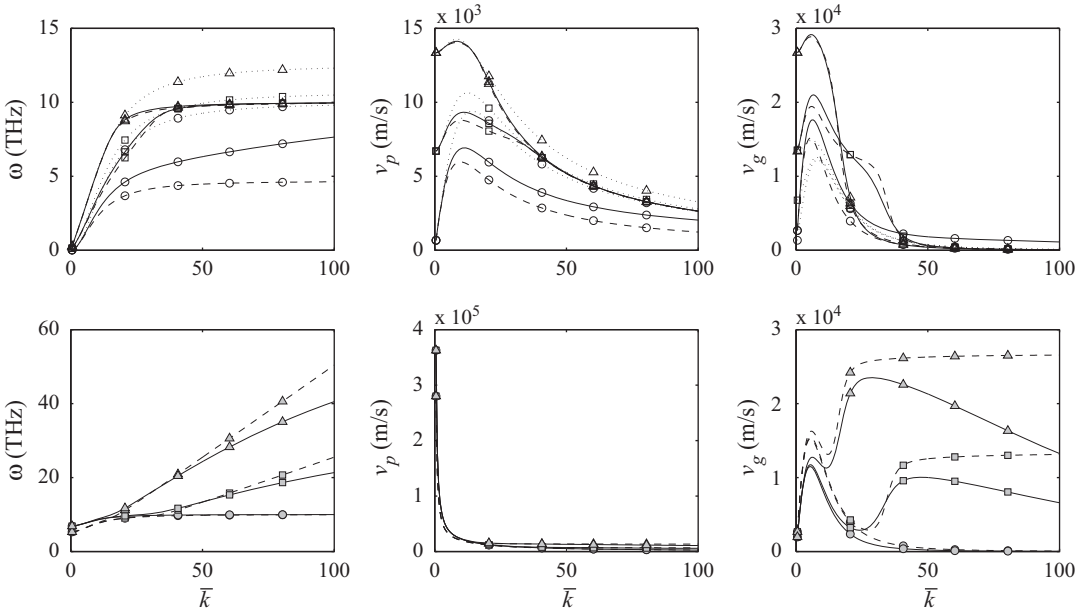

Fig. 4. Plots of dispersion curves, phase velocities, and group velocities for different levels of axial magnetic field ((○) $\overline{H}_x^R=0$, (□) $\overline{H}_x^R=5$, (△) $\overline{H}_x^R=10$; (...) NRBT, (– · –) NTBT, (—) NHOBT; $\lambda=15$, $e_0a=2$ nm, $K_r=K_t=0$).

wavenumber (i.e., $\overline{k}=\pi,5\pi$,and 10π). As it is obvious in Fig. 5, both flexural and shear frequencies as well as their corresponding phase velocities generally increase with the longitudinal magnetic field. In the cases of $\overline{k}=5\pi$ and 10π, the flexural frequencies and their corresponding phase velocities of the nonlocal shear deformable beams do not alter for a longitudinal magnetic field greater than a certain value. As it is also seen in Fig. 5, the predicted flexural frequencies and phase velocities are overestimated by the NRBT, particularly for high levels of the longitudinal magnetic field and the wavenumber. For the considered wavenumbers, the predicted shear frequencies as well as the corresponding phase and group velocities of the NTBT and the NHOBT are generally in line. The predicted shear group velocities by the nonlocal shear deformable beams increase with the applied axial magnetic field. The predicted flexural group velocities by the NRBT commonly increase with the longitudinal magnetic field as well. However, the flexural group velocity plot of each nonlocal shear deformable beam has its own peak point, and its maximum value magnifies with the wavenumber.

Another important inspection should be undertaken to realize the effect of the small-scale parameter on the characteristics of the propagated transverse waves within SWCNTs under an axial magnetic field. To this end, the plotted results of the frequencies, phase velocities, and group velocities of the propagated waves within the SWCNT are demonstrated in Fig. 6 for different levels of the axially applied magnetic field. As it is seen in Fig. 6, the predicted flexural and shear frequencies generally decrease with the small-scale parameter, irrespective of the assumed level of the

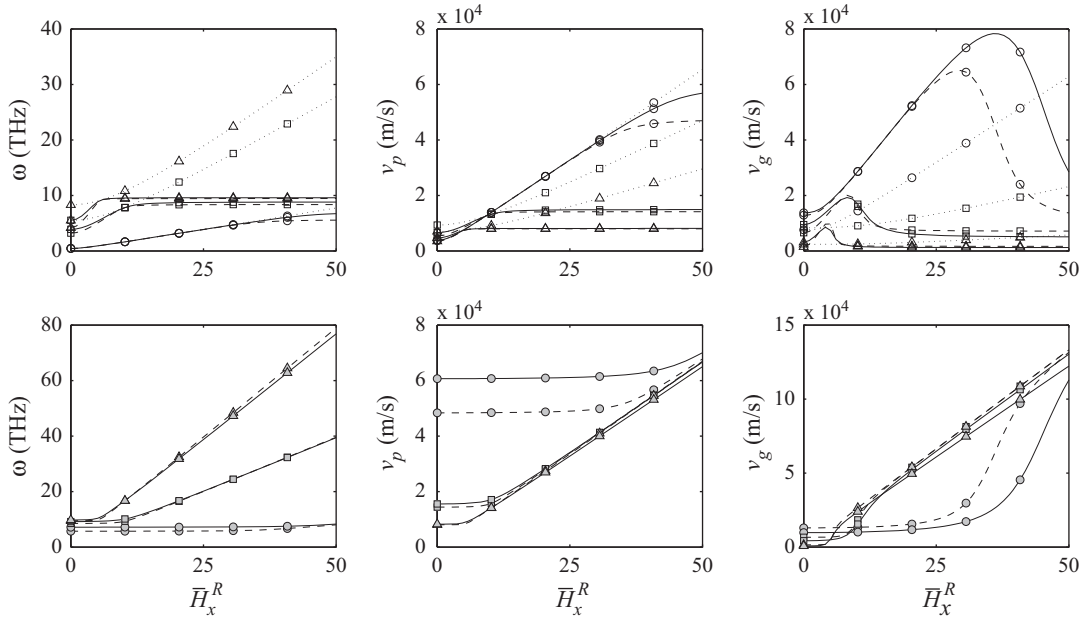

Fig. 5. Variation of frequencies, phase velocities, and group velocities as a function of normalized axial magnetic field for different dimensionless wavenumbers ((○) $\overline{k}=\pi$, (□) $\overline{k}=5\pi$, (△) $\overline{k}=10\pi$; (...) NRBT, (− · −) NTBT, (—) NHOBT; $\lambda=15$, $e_0a=2$ nm, $K_r=K_t=0$).

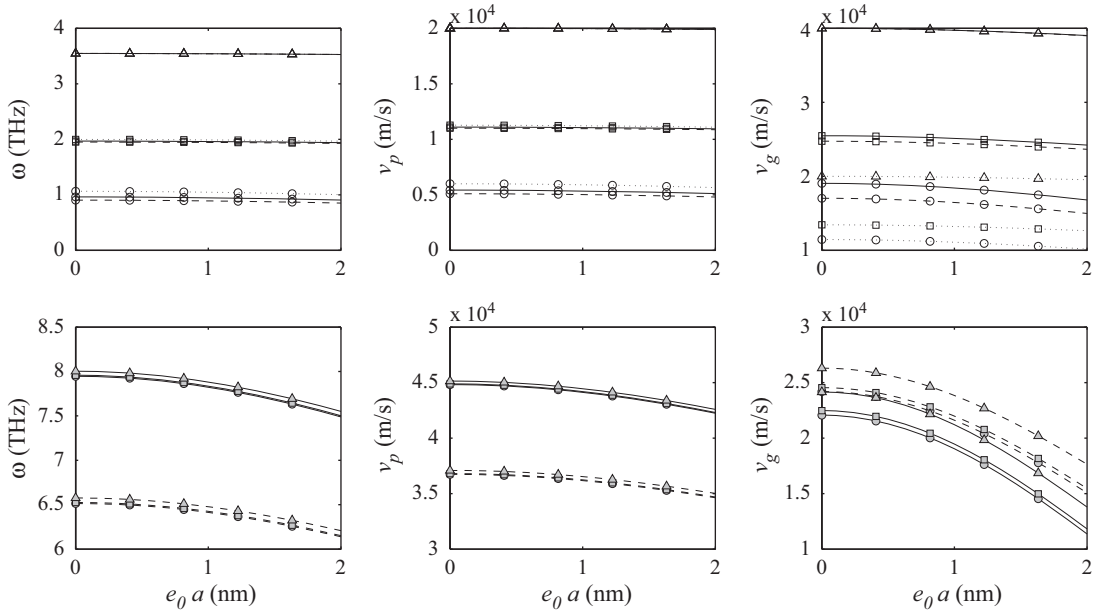

Fig. 6. Variation of frequencies, phase velocities, and group velocities corresponding to $\overline{k}=\pi$ as a function of small-scale parameter for different levels of axial magnetic field ((○) $\overline{H}_x^R=0$, (□) $\overline{H}_x^R=5$, (△) $\overline{H}_x^R=10$; (...) NRBT, (− · −) NTBT, (—) NHOBT; $\lambda=15$, $e_0a=2$ nm, $K_r=K_t=0$).

longitudinal magnetic field. Additionally, phase velocities as well as group velocities of the proposed models would reduce as the influence of the small-scale parameter becomes highlighted. For an assumed level of the applied longitudinal magnetic field, the effect of the small-scale parameter on the characteristics associated with the shear waves is more obvious with respect to those pertinent to the flexural waves.

The influence of the lateral stiffness of the surrounding matrix on the characteristics of the sound waves within SWCNTs subjected to a longitudinal magnetic field is of concern. In Fig. 7, the graphs of the frequencies, phase velocities, and group velocities associated with $\overline{k}=\pi$ as a function of dimensionless lateral stiffness of the surrounding elastic medium are presented for different levels of the longitudinal magnetic field. The results are provided for a SWCNT with $\lambda=15$ and $e_0a=2$ nm when the surrounding medium does not resist the rotation of the embedded SWCNT. As it is seen in Fig. 7, the flexural frequencies and the corresponding phase velocities would increase with the lateral stiffness of the surrounding matrix. Moreover, the predicted group velocities would generally decrease with the lateral stiffness of the surrounding elastic medium. As the effect of the lateral stiffness of the surrounding matrix becomes highlighted, the discrepancies between the results of the NRBT and those of the nonlocal shear deformable models decrease. For an assumed level of the longitudinally applied magnetic field, both the NTBT and the NHOBT predict that the variation of the lateral stiffness of the elastic matrix has fairly no effect on the variation of the characteristics pertinent to the propagated shear waves within the SWCNT.

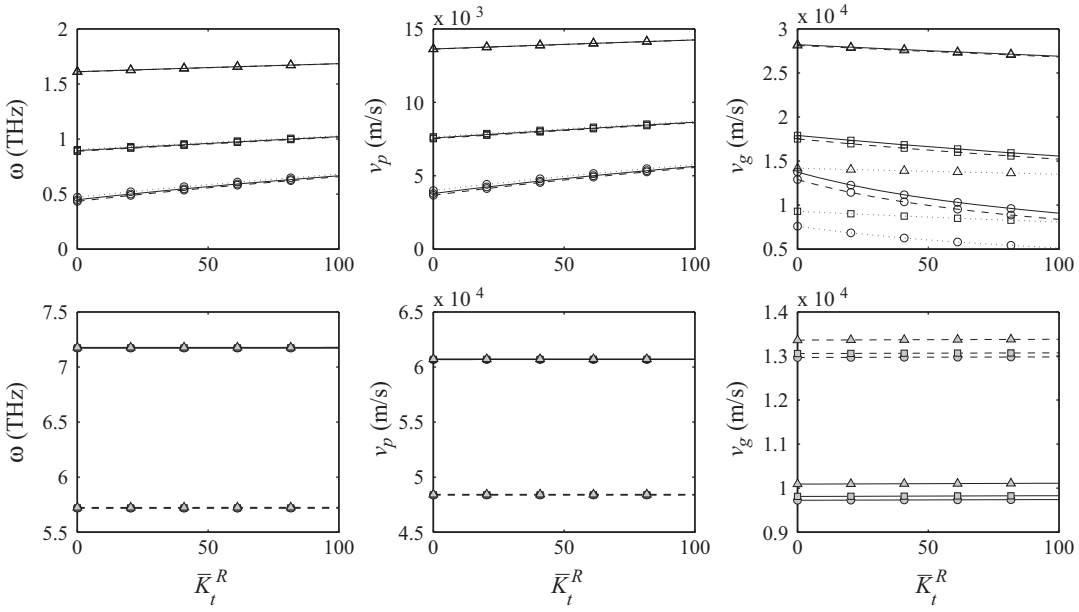

Fig. 7. Variation of frequencies, phase velocities, and group velocities pertinent to $\overline{k}=\pi$ in terms of normalized lateral stiffness of the surrounding matrix for different dimensionless wavenumbers ((○) $\overline{H}_x^R=0$, (□) $\overline{H}_x^R=5$, (△) $\overline{H}_x^R=10$; (...) NRBT, (− · −) NTBT, (—) NHOBT; $\lambda=15$, $e_0a=2$ nm, $K_r=0$).

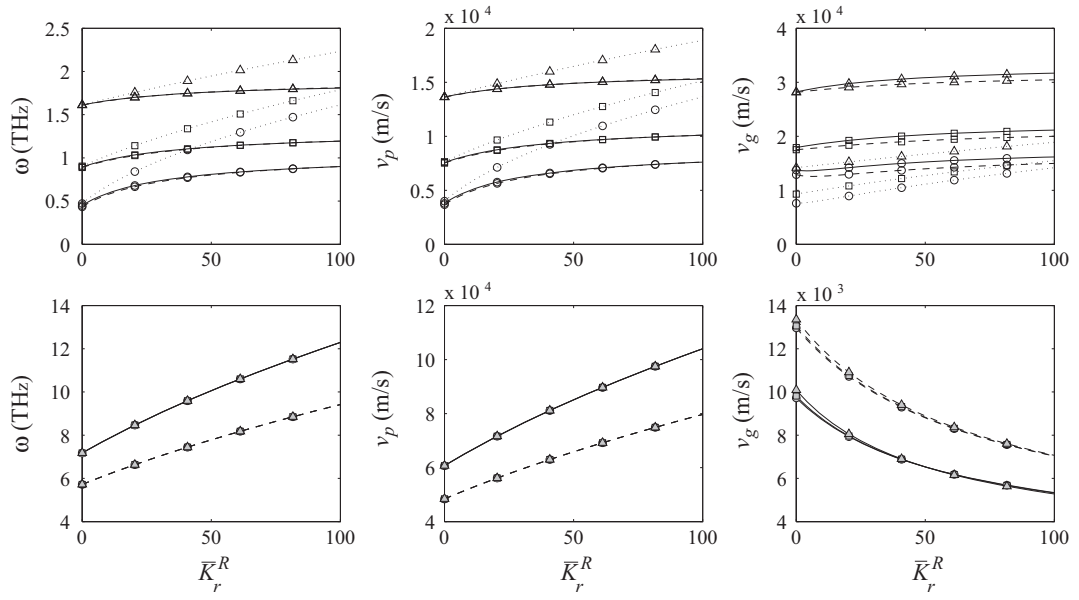

Fig. 8. Variation of frequencies, phase velocities, and group velocities pertinent to $\overline{k}=\pi$ in terms of normalized rotational stiffness of the surrounding matrix for different dimensionless wavenumbers ((○) $\overline{H}_x^R=0$, (□) $\overline{H}_x^R=5$, (△) $\overline{H}_x^R=10$; (...) NRBT, (− · −) NTBT, (—) NHOBT; $\lambda=15$, $e_0a=2$ nm, $K_t=0$).

Finally, the effect of the rotational interaction of the surrounding elastic matrix with the SWCNT on the characteristics of the propagated waves within SWCNTs subjected to a longitudinal magnetic field is of particular significance. In Fig. 8, the frequencies, the phase velocities, and the group velocities of the transversely propagated waves within SWCNTs in terms of the rotational stiffness of the surrounding matrix have been presented. The results are given for a SWCNT with $\lambda=15$ and $e_0a=2$ nm when the surrounding elastic medium does not prevent the SWCNT from lateral vibration (i.e., $K_t=0$). As it is obvious in Fig. 8, the flexural frequencies as well as the corresponding phase and group velocities of the nonlocal beams generally magnify with the rotational stiffness of the elastic matrix. The NRBT overestimates the flexural frequency and the corresponding phase velocity with respect to the NTBT and the NHOBT. Moreover, the discrepancies between the results of the NRBT and those of the nonlocal shear deformable beams generally increase with the rotational stiffness of the surrounding matrix. A scrutiny of the plotted results reveals that the discrepancies between the predicted flexural frequencies by the NTBT and those of the NHOBT would generally lessen as the rotational interaction of the SWCNT with its surrounding matrix intensifies. Conversely, the discrepancies between the predicted shear frequencies (and also the shear phase velocities) by the NTBT and those of the NHOBT would commonly amplify with the rotational stiffness of the surrounding matrix. Further, the predicted shear group velocities by the nonlocal shear deformable beam models decrease with the rotational stiffness of the surrounding matrix.

8. Concluding remarks

The transverse wave propagation within elastically confined SWCNTs under a longitudinal magnetic field is investigated through some nonlocal beam models. The SWCNT is modeled as a hollow cylinder and its interactions with the surrounding medium are taken into account by lateral and rotational continuous springs. The effect of the longitudinal magnetic field on the generated forces in the ECS is considered via appropriate Lorentz's forces. For each model, the dispersion relation of the transverse waves is derived. For the NRB under an axial magnetic field, only one frequency is detected; however, two frequencies are recognized for the nonlocal shear deformable beams: one frequency is pertinent to the flexural wave mode and the another one is related to the shear wave mode. Using the obtained dispersion relations, the explicit expressions of frequencies, phase velocities, and group velocities of the shear and flexural waves are obtained for the proposed models. Subsequently, the effects of slenderness ratio, small-scale parameter, longitudinal magnetic field, mean radius of the ECS, lateral and rotational stiffness of the surrounding matrix on the characteristics of the propagated waves are examined in some details. The main results are as follows:

- In all proposed models, an increase of the longitudinally applied magnetic field would result in the increase of the predicted flexural and phase velocities. This fact is more noticeable for SWCNTs with low levels of the slenderness ratio.
- As the mean radius of the SWCNT increases, the discrepancies between the flexural frequencies as well as the phase velocities of the NRB and those of the nonlocal shear deformable beams increase. The overall behavior of the flexural frequencies of the proposed models as a function of radius of the SWCNT highly depends on the level of the axial magnetic field.
- In most of the cases, the predicted dispersion curve by the NHOBT has been somehow placed between that of the NRBT and that of the NTBT. The NRBT commonly overestimates the flexural frequencies and phase velocities, irrespective of the axial magnetic field. Additionally, the discrepancies between the results of the NRBT and those of the nonlocal shear deformable beams generally intensify with the wavenumber. As the longitudinal magnetic field magnifies, the discrepancies between the shear group velocities of the NTBT and those of the NHOBT generally amplify.
- Generally, both flexural and shear frequencies as well as their corresponding phase and group velocities decrease with the small-scale parameter, irrespective of the level of the longitudinal magnetic field. As the longitudinal magnetic field increases, the sensitivity of the predicted flexural frequency and the phase velocity to the small-scale parameter would lessen.
- The discrepancies between the results of the NRBT and those of the nonlocal shear deformable beam models decrease as the lateral stiffness of the surrounding elastic medium increases. The predicted flexural frequencies and the pertinent phase velocities of various nonlocal beam models increase with the lateral stiffness; however, the predicted group velocities reduce as the lateral stiffness becomes highlighted.
- The flexural frequencies and the corresponding phase and group velocities would increase as the rotational stiffness of the surrounding matrix increases. The shear frequencies and the corresponding phase velocities of the nonlocal shear deformable beams also increase with the rotational stiffness; however, the group velocities corresponding to the shear waves decrease with the rotational stiffness. Furthermore, the discrepancies between the flexural frequencies of the NRBT and those of the nonlocal shear deformable beam models generally increase as the rotational interaction of the SWCNT with its surrounding medium intensifies.

References

[1] H. Ajiki, T. Ando, Journal of Physical Society of Japan 62 (1993) 1255.
[2] H. Ajiki, T. Ando, Physica B 201 (1994) 349.
[3] H. Ajiki, T. Ando, Journal of Physical Society of Japan 65 (1996) 505.
[4] R. Saito, G. Dresselhaus, M.S. Dresselhaus, Physical Properties of Carbon Nanotubes, Imperial College Press, London, 1998.
[5] M.J. Óconnell, Carbon Nanotubes: Properties and Applications, CRC Press, Boca Raton, 2006, pp. 119–151.
[6] Y. Aharonov, D. Bohm, Physical Review 115 (1959) 485.
[7] T. Ando, Role of the Aharonov-Bohm phase in the optical properties of carbon nanotubes, Topics in Applied Physics, Springer Publisher, Heidelberg, 2008, pp. 229–250.
[8] J. Kono, R.J. Nicholas, S. Roche, High magnetic field phenomena in carbon nanotubes, Topics in Applied Physics, Springer Publisher, Heidelberg, 2008, pp. 393–421.
[9] M. Fujiwara, E. Oki, M. Hamada, Y. Tanimoto, I. Mukouda, Y. Shimomura, Journal of Physical Chemistry A 105 (18) (2001) 4383.
[10] M.A.C. Duarte, M. Grzelczak, V.S. Maceira, M. Giersig, L.M.L. Marzan, M. Farle, K. Sierazdki, R. Diaz, Journal of Physical Chemistry B 109 (41) (2005) 19060.
[11] H. Lu, J. Gou, J. Leng, S. Du, Applied Physics Letters 98 (2011) 174105.
[12] E. Camponeschi, R. Vance, M. Al-Haik, H. Garmestani, R. Tannenbaum, Carbon 45 (2007) 2037.
[13] K. Bubke, H. Gnewuch, M. Hempstead, J. Hammer, M.L.H. Green, Applied Physics Letters 71 (14) (1997) 1906.
[14] X. Liu, J.L. Spencer, A.B. Kaiser, W.M. Arnold, Current Applied Physics 4 (2004) 125.
[15] C. Sun, K. Liu, Solid State Communications 143 (4–5) (2007) 202.
[16] L.L. Ke, Y. Xiang, J. Yang, S. Kitipornchai, Computational Materials Science 47 (2) (2009) 409.
[17] K.B. Mustapha, Z.W. Zhong, Computational Materials Science 50 (2) (2010) 742.
[18] R.D. Firouz-Abadi, A.R. Hosseinian, Computational Materials Science 53 (1) (2012) 12.
[19] K. Kiani, International Journal of Mechanical Sciences 52 (10) (2010) 1343.
[20] L.L. Ke, J. Yang, S. Kitipornchai, Composite Structures 92 (3) (2010) 676.
[21] S. Arghavan, A.V. Singh, Journal of Sound and Vibration 330 (13) (2011) 3102.
[22] M. Janghorban, A. Zare, Physica E 43 (9) (2011) 1602.
[23] J. Yoon, C.Q. Ru, A. Mioduchowski, Composites Part B: Engineering 35 (2) (2004) 87.
[24] Q. Wang, G.Y. Zhou, K.C. Lin, International Journal of Solids and Structures 43 (20) (2006) 6071.
[25] Q. Wang, V.K. Varadan, International Journal of Solids and Structures 43 (2) (2006) 254.
[26] K.M. Liew, Q. Wang, International Journal of Engineering Science 45 (2–8) (2007) 227.
[27] K. Dong, S.Q. Zhu, X. Wang, Composite Structures 82 (1) (2008) 1.
[28] H. Heireche, A. Tounsi, A. Benzair, M. Maachou, B.E.A. Adda, Physica E 40 (2008) 2791.
[29] H. Heireche, A. Tounsi, A. Benzair, Journal of Applied Physics 104 (2008) 104301.
[30] J. Yoon, C.Q. Ru, A. Mioduchowski, Composites Science and Technology 65 (9) (2005) 1326.
[31] Y. Yan, X.Q. He, L.X. Zhang, C.M. Wang, Journal of Sound and Vibration 319 (3–5) (2009) 1003.
[32] L. Wang, Physica E 43 (1) (2010) 437.
[33] L. Wang, Journal of Fluids and Structures 26 (4) (2010) 675.
[34] L.L. Ke, Y.S. Wang, Physica E 43 (5) (2011) 1031.
[35] A. Tounsi, H. Heireche, E.A. Adda Bedia, Journal of Applied Physics 105 (2009) 126105.
[36] A. Tounsi, H. Heireche, A. Benzair, I. Mechab, Journal of Physics: Condensed Matter 21 (44) (2009) 448001.
[37] K. Kiani, Vibration behavior of simply supported inclined single-walled carbon nanotubes conveying viscous fluids flow using nonlocal Rayleigh beam model, Applied Mathematical Modelling http://dx.doi.org/10.1016/j.apm.2012.04.027, 2012.
[38] K. Kiani, B. Mehri, Journal of Sound and Vibration 329 (11) (2010) 2241.
[39] K. Kiani, Physica E 42 (9) (2010) 2391.
[40] K. Kiani, Acta Mechanica 216 (2011) 165.
[41] K. Kiani, Acta Mechanica 216 (2011) 197.
[42] K. Kiani, Q. Wang, European Journal of Mechanics A/Solids 31 (1) (2012) 179.
[43] H. Wang, K. Dong, F. Men, Y.J. Yan, X. Wang, Applied Mathematical Modelling 34 (2010) 878.
[44] S. Li, H.J. Xie, X. Wang, Bulletin of Materials Science 34 (1) (2011) 45.
[45] X. Wang, J.X. Shen, Y. Liu, G.G. Shen, G. Lu, Applied Mathematical Modelling 36 (2) (2012) 648.
[46] A.C. Eringen, Journal of Mathematics and Mechanics 15 (1966) 909.
[47] A.C. Eringen, International Journal of Engineering Science 10 (1972) 1.
[48] A.C. Eringen, Nonlocal Continuum Field Theories, Springer-Verlag, New York, 2002.
[49] W.H. Duan, C.M. Wang, Y.Y. Zhang, Journal of Applied Physics 101 (2007) 024305(1).
[50] J.D. Kraus, K.R. Carver, Electromagnetics, second ed., McGraw-Hill, 1981.
[51] J.F. Doyle, Wave Propagation in Structures, second ed., Springer-Verlag, New York, 1997.